Form-Finding and Structural Shape Optimization of the Metal 3D-Printed Multi-Branch Node with Complex Geometry

Vahid Hassani[1] [ID], Zubin Khabazi[2] [ID], Felix Raspall[3] [ID], Carlos Banon[4] [ID] and David W.Rosen[5] [ID]

[1]Singapore University of Technology and Design, dr.vahid.hassani@gmail.com
[2]Singapore University of Technology and Design, zubin@morphogenesism.com
[3] Singapore University of Technology and Design, felix_raspall@sutd.edu.sg
[4] Singapore University of Technology and Design, carlos_banon@sutd.edu.sg
[5] Singapore University of Technology and Design, david_rosen@sutd.edu.sg

Corresponding author: Vahid Hassani, dr.vahid.hassani@gmail.com

Abstract. The application of additive manufacturing (AM) technology in architecture and structural engineering has been extended due to recent development of metal 3d printing. In space frame structures, a set of bars is configured in three dimensions, with bars connected by nodes. This article presents two methods to design metal 3d-printed multi-branch nodes to accommodate any number of incident bars at arbitrary angles. Resulting node designs are intended to be smooth and lightweight. A multi-branch node is sketched using the dimensional information of the blank space between the converging bars in a pre-designed space frame and then parameterized by two different approaches to perform structural optimization. The first design method, namely the curve parameter method, which is semi-automated approach, the distances between the control points of the spline curves between node branches and the node branch intersection point are the optimization parameters. For the other method, called fatness parameter method, which is a fast and automated approach, the fatness parameters of the center part of the node and the root radiuses of each branch are chosen as the main parameters of optimization. The optimization procedure is accomplished using a genetic algorithm to minimize the maximum von Mises stress as the objective function subjected to the mass of the node as a constraint function. Finally, functional tests are conducted on 3D printed metal nodes in order to compare the strength and stiffness of the nodes designed by the two form-finding approaches.

Keywords: Form-Finding, Structural Optimization, Curve Parameter Method, Fatness Parameter Method, Metal 3d-Printing, Space Frame Node
DOI: https://doi.org/10.14733/cadaps.2020.205-225

1   INTRODUCTION

In the last few years, considerable attention has been paid to additive manufacturing (AM) technologies [12] to redesign and modify the industrial products with regard to its merits. At the initial stage of technology development, AM was mostly used as a building platform for

prototyping, whereas its usage has been recently extended to industrial applications. Amid the different methods of AM technology, the development of metal AM, in particular, Powder Bed Fusion (PBF) and metal Binder Jetting, facilitate the production of high-quality and complex parts in several sectors of industry such as aerospace, medical, architecture and civil engineering. Understanding the novel advantage of metal 3d-printing in the development of high-performance and functional parts for applications in the construction sector enables researchers to propose plenty of shape optimization algorithms to maximize structural, material and spatial performance of buildings, however due to novelty of metal 3d-printing technology, its application in architecture and civic sectors remains largely unexplored.

Among the different types of built constructions, space frames (SFs) have attracted much interest across the world due to their simpler structure, lower costs and faster build process compared to the conventional counterparts. This type of construction consists of nodes and bars organized into three-dimensional configurations. The focus of research in recent years has been mostly on the form-finding of such kind of constructions entirely in a specific volume with regards to a number of target variables such as span, weight, cost, compliance, etc. In the literature, several methods have been devoted to the form-finding of SF configurations regardless of the single constitutive components of such construction. Nevertheless, the algorithms proposed for the whole structure can be generalized to design and development of single components. One of the first examples of form-finding algorithms is presented for the analytical shape finding of cable nets [14]. Then this research was continued more systematically by introducing the three basic algorithms namely, force density method [28], dynamic relaxation method and updated reference strategy [4]. In order to have a broader study on different methods of form-finding, readers may refer to [30]. An alternative form-finding technique was proposed for three-dimensional spatial structures based on the minimization of the strain energy subjected to mass constraint [17]. Two different techniques, one based on the genetic algorithm and the other based on the algebraic method, were also developed for the form-finding of tensegrity structures [10] that have large applications in civil structures [11], space structures [13] and robotics [22].

On top of the form-finding methods of SF's, several publications have appeared in recent years documenting the structural shape optimization [2-3] of discrete structures and mechanical systems. As some examples of the research presented in this field, one can find the node-shifting method, which has been used to enhance the structural stiffness of spatial structures [7], metaheuristic algorithms for multi-objective optimization of a drill geometry to increase its mechanical performance [1], shape and size optimization of a roof structure and its members by using the two-phase genetic algorithm and evolutionary computing [16], multi-objective genetic algorithm for grid homogenization of a grid-shell structure to vary rod directions on the shell surface in response to one or more load cases [34], and genetic algorithm and associative parametric based optimization for complex spatial structures [5].

The vast variety of approaches has been proposed to solve the structural shape optimization problem of discrete structures and mechanical systems. For instance, the other approach that has attracted much attention from research teams is the structural shape optimization by non-uniform rational B-spline (NURBS) modeling. Noel et al. [21] published one of the most fundamental researches in which the B-Rep modelling technique forms the basis for the part geometry parameters. Further, these parameters are updated based on the gradient method in order to complete the optimization loop for both the objective and constraint functions. Similarly, a chain link was parameterized by B-spline functions and optimized in terms of two dimensional problem [32]. Using the concept of freeform surfaces results in a reduced number of parameters and less computational time for the optimization process, accordingly. Generally, the main goal of research in the field of NURBS modeling pivots about a center to reduce the number of parameters and computational time for a particular problem. A feature-based geometry creation and optimization approach for structure design was studied in [33]. In other research, NURBS surfaces were used to describe the geometry cross-section of axisymmetric solid parts and the shape optimization process was completed by sequential quadratic programming algorithm [18]. Marco et al. [19] merged the immersed boundary methods and NURBS-Enhanced finite element method to create

adaptive mesh for moving the geometry boundary to obtain the structurally optimized configuration of a solid part. NURBS modeling is not only used to represent the geometry of the solid parts, but also it has application to obtain the optimum configuration of truss structures [8] and trimmed shell structures [15].

To the authors' knowledge, the design methodology and shape optimization of SF nodes with irregular and complex geometry has only recently been investigated from the aspect of the possibility of metal AM in the building industry [9], [20]. As discussed earlier, one of the main advantages of AM technology, in particular metal 3d-printing, is to create solid parts with complex geometry, lower weight and higher performance in comparison with the original parts.

On the continuation of previous researches, this research aims to propose two design methods for the SF's nodes that possess irregular shapes with complex geometry. These methods namely, the curve parameter method and the fatness parameter method, rely on the particular capabilities of CAD software to sketch the original part, parameterization of the geometry and finally structural shape optimization of the part. The former method takes longer time to be completed while the latter one is faster. In contrast to the NURBS models, these methods are acclaimed due to their less computational time, less complexity of the model and more scalability. The manufacturability of the final parts is also considered in metal AM framework and the performance of each part is analyzed by functional testing.

The remainder of the paper is organized as follows. In Section 2, the background, applications and benefits of the proposed nodes are described in detail. In Section 3, the curve parameter method will be discussed. Afterward, the fatness parameter method is presented in Section 4. Section 5 compares the two parts in terms of performing functional testing. Some conclusions will be wrapped up in Section 6.

2   BACKGROUND, APPLICATIONS AND BENEFITS

Through the progress of AM technologies in recent years, researchers and industries have focused on redesign and development of functional and more specific products in different industry sectors. This is because AM offers some unique capabilities and design freedoms compared to conventional manufacturing methods. These capabilities are mainly manifested in terms of customized products with shape, material, hierarchical and functional complexities [26]. Notwithstanding, the use of AM is limited in some sectors due to small build volume and high operation costs. Considering the current capabilities and shortcomings of AM technologies will give a roadmap to both researchers and industries to redesign end-use parts to be more functional and specific in comparison with those that were manufactured by conventional methods.

One of the industry sectors in which AM can play a key role is the civic industry. Amid the myriads of civic buildings, SFs are enumerated due to their wide applications for building the stations, pavilions, sport complexes, museums,etc. These structures are designed by using some algorithms like vMESH system [25,31] by which a tetrahedral three-dimensional mesh is generated from a given prismatic volume. The resultant randomly generated graph–shaped structures will give the dimensional information such as bar orientations and initial nodes topologies (see Figure 1(a), Figure 1(b)). Since the generated wireframe structure has random shape, the connecting nodes also have unique and irregular configuration as seen in Figure 2(a), Figure 2(b).

For development of such structures, AM technologies, particularly metal AM, can ensure promising results because [24]:
1. SFs, which are generated by vMESH system, consists of two main elements namely, bars and nodes. The former is made of metal, cylindrical shape, and economically and practically unjustifiable to be manufactured by AM, while the latter has complex shape and has to be built by AM.
2. Wireframe SF enables the construction designers to use the specific and limited space more efficiently with more expressive quality and flexibility, overcoming the unpleasant appearance

of the hidden SF under cladding and the ugly welded joints like shown in Figure 3(a), Figure 3(b).

3. Nodes in SFs can be customized through AM and the efficiency of the structure can be increased.

Figure 1: From left to right. (a) vMESH Light Network, (b) vMESH Table Structure.
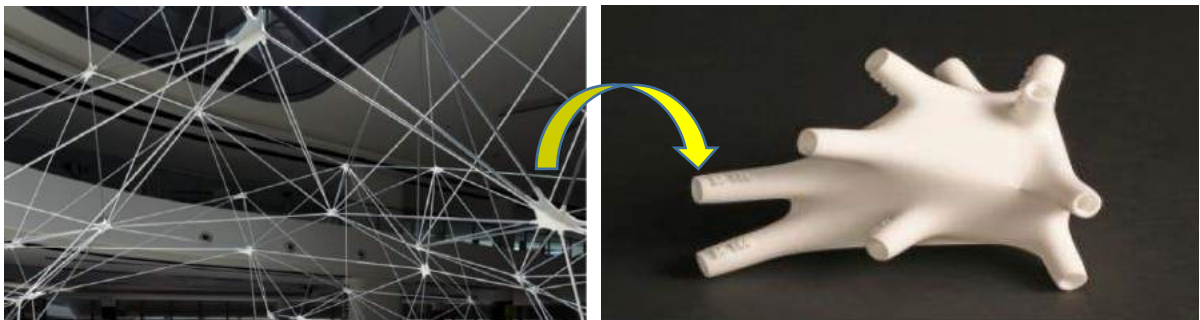
Figure 2: From left to right. (a) SF Generated by vMESH System, (b) Close-up View of the Node with Unique Configuration.

Figure 3: From left to right. (a) SF under Cladding, (b) Poor Appearance of Welded Joint in Conventional SF.

In addition to civic sector, SFs can be used alternatively in another industry sectors such as aerospace, automotive, motorcycle, and even bicycle. The internal structure of an aircraft and some car designs consists of some lateral and longitudinal elements which are well-known as bulkhead frames, spars, stingers and longerons. These elements, either welded or riveted, will define the external configuration of aircrafts and cars. Novel SF designs can give motorcycles and bicycles striking appearances with good performance, which requires new node design approaches.

In former research [24-25], after generating the mesh structure systematically by using the vMESH method, designer had to design nodes manually, which was time consuming for one node and tedious since each node had a unique shape. Each node could require 5-10 hours to manually design. To address the issue, this research aims to use two approaches for creating the nodes more systematically. These approaches enable the researchers to design and optimize node geometry using geometric modeling and structural shape optimization technologies, respectively.

The advantages, which are offered by the new node configuration and new design approaches, are listed as follows:
1. The new design is able to carry both compression and tensile loads.
2. The new design will give more freedom to designers to create different configurations of SF structures.
3. These nodes are not only used for joining the members in SF, but could be used to connect the pipelines with complex grid networks in hydraulic and pneumatic systems.
4. It is easy to be geometrically parameterized and structurally optimized.
5. Most AM processes can fabricate these nodes with unique features.

All types of connections such as weld joint, screw joint and pin joint are applicable to the new node system.

3   CURVE PARAMETER METHOD

This section is devoted to describe the curve parameter method for designing the SF's nodes in three steps. These steps, namely node sketching, parameterization and structural optimization, are comprehensively discussed as follows and can be applied to all types of nodes which belongs to the class of node as shown in Figure 2(b). The design method was implemented using three software packages, with LiveLink interfaces among them: SOLIDWORKS, MATLAB and COMSOL. The digital workflow between these software packages starts with SolidWorks, where initial sketching and parameterization is performed, then transitions to COMSOL for FEA.

3.1   Node Sketching

The design process is started by sketching the initial configuration of a SF's node, based on the number of bars converging to that node and their angles. Bar radius is selected for the SF and that radius becomes the radius of the cylinders generated for the node. An example sketch for a node with 10 incident bars is in Figure 4.
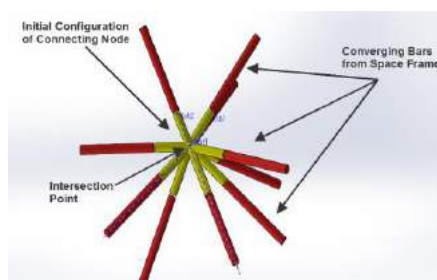
Figure 4: Initial configuration of the connecting node and converging bars.

Node designs are intended to have smooth shapes. A smooth curve is constructed between each pair of neighboring cylinders. To construct this curve, a straight line called the upper line is constructed between the cylinder centers. Then, the center of this line is connected to the intersection point by a perpendicular line. All these elements are shown in Figure 5.
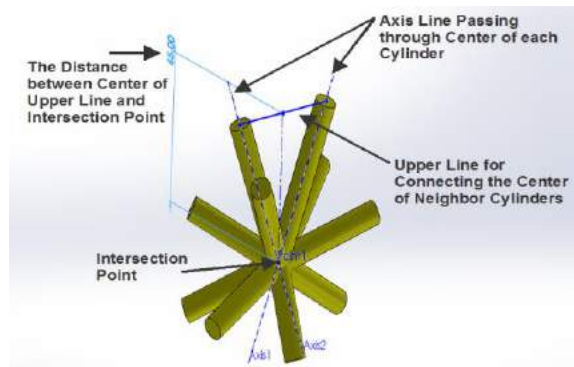
Figure 5: Two axis lines and the straight upper line for connecting the center of each cylinder.

The mid-point between the center of the upper line and the intersection point is chosen as a control point to initiate the sketching of the "Style Spline" (Bezier curves in SolidWorks) curve between two cylinders. Figure 6 illustrates the starting point of the spline curve at the aforementioned distance to the intersection point.

For every three neighboring cylinders, a smooth surface will be constructed to form the body of the node. Spline curves are created between all three pairs of neighboring cylinders, then a filling surface is created by connecting the three spline curves. Figure 7 shows the resultant surface from three spline curves. Note that the designer performs these construction steps.

After completion of drawing filling surfaces for all neighboring cylinders, the boundaries of surfaces are knitted to each other and the internal section of the node is converted to solid. Before conversion to solid part, the parameterization step has to be performed described as follows.
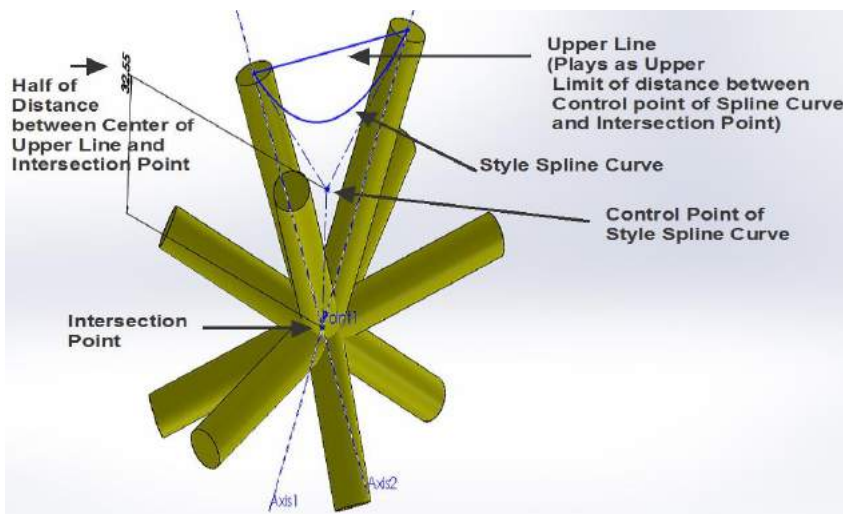
Figure 6: Spline curve and its control point.

Three Spline Curves

Resultant
Surface from
Three Spline
Curves
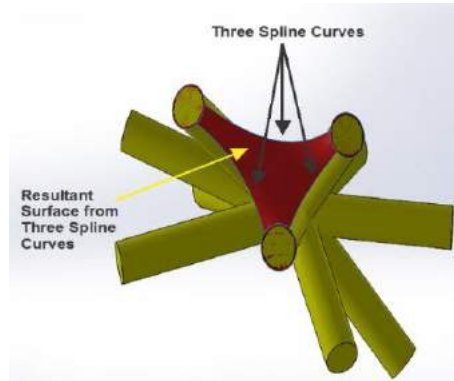
Figure 7: Resultant surface from three spline curves.

3.2 Node Parameterization

Once the drawing of spline curves and filling surfaces is completed, the parameterization step is commenced sequentially. Prior to parameter selection, it should be noted that the intersected cylinders will be converted to solid structure after creating the filling surfaces through the spline curves. Therefore, the cylinders do not have a significant role in the shape of the node at the end of the drawing process. With this in mind, the main feature that forms the final configuration of the node is the concavity of the spline curves. Increased concavity of the spline curves yields a slim node, while the less concavity results in fatter node (see Figure 8(a), Figure 8(b)). In order to control the concavity of the curves, the distances between control points of each spline curve and the intersection point are chosen as design parameters of the node. These distances are constrained between lower and upper limits. Figure 9(a) shows the upper limit of the spline curve with less concavity, whereas Figure 9(b) shows the lower limit of the curve with more concavity. Note should be taken that the lower limit is set 1mm between the control point of the curve and the intersection point for all spline curves of the neighboring cylinders and the upper limit is chosen such that the minimum concavity of the curve is ensured.
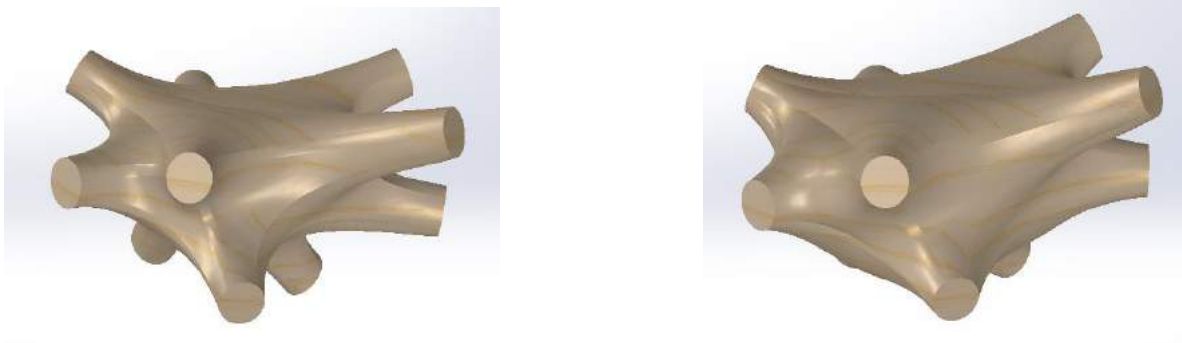
Figure 8: From left to right. (a) Slim Node with Higher Concavity of the Spline Curves, (b) Fat Node with Smaller Concavity of the Spline Curves.
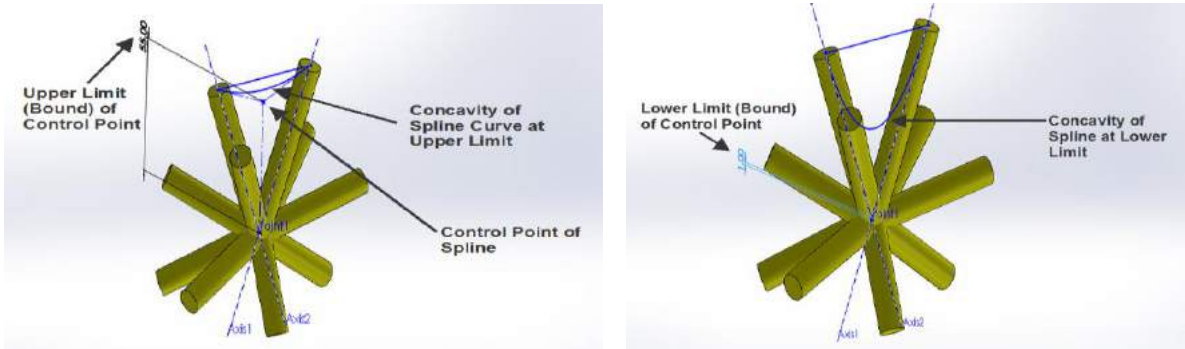
Figure 9: From left to right. (a) Upper Limit of the Curve with Minimum Concavity, (b) Lower Limit of the Curve with Maximum Concavity.

3.3 Node Structural Optimization

After determination of the design variables in terms of node parameters, the structural shape optimization problem can be solved to optimize node shape using the control points of the splines in the design variables. In this research, the objective function was to minimize the maximum von Mises stress of the node, subject to a mass constraint. This objective was chosen so that we had direct control over stresses and the node's factor of safety. We wanted to explore the behavior of this objective function. Note the use of a mass (or volume) constraint is consistent with topology optimization formulations. Design variables are the distances between the ith spline control point and the center of the node, called the intersection point. The structural optimization problem formulation is given in Table 1.

Given	B.C, Loads, Material
Find	D_i: The ith distance between control point of ith spline and intersected point
Satisfy	$D_i^l \leq D_i \leq D_i^u$: Lower and upper bounds of distances between control points and intersected points
	$M_{total\_mass} \leq M_{target}$: Maximum total mass of the node
Minimize	Max $\sigma_{von Mises}$: Maximum von Mises Stress

Table 1: Formulation of optimization problem.

Given the boundary conditions, B.C, loads and material information, the distances between the control points of spline curves and intersected point, D_i, will be optimized. The threshold node mass value, M_{target}, is selected based on the structural system requirements and the structural characteristics of the specific node. Von Mises stresses are determined using finite element analysis (FEA). By setting the initial values of design parameters, $D_i's$ in the middle of their lower and upper bounds, FEA was performed using the COMSOL software. COMSOL meshed node geometry at each iteration using the "extremely fine" setting. Linear tetrahedral elements were used. Point loads were applied in the center of the circular faces along the branch center-lines. Their magnitudes are shown in Figure 10. These loads were calculated using a separate analysis on vMESH in Karamba software [23]. The material was chosen to be MaragingSteel MS1 for EOS M280 metal 3d-printers. The mechanical properties for the material are given in Table 2.
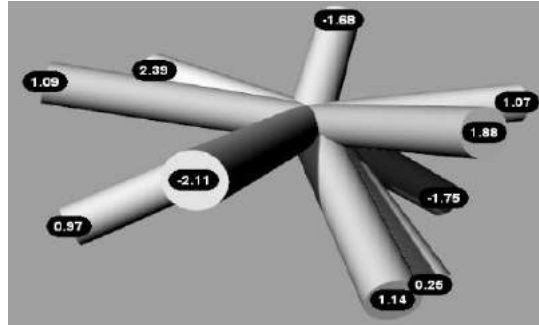
Figure 10: Load applied on each branch's surface (KN).

Mechanical Properties	Quantity
Young's Modulus	177 GPa
Yield Strength	1000 MPa
Tensile Strength	1150 MPa
Poisson's Ratio	0.33
Density	8000 kg/m^3

Table 2: Mechanical properties of Maraging Steel MS1 metal powder.
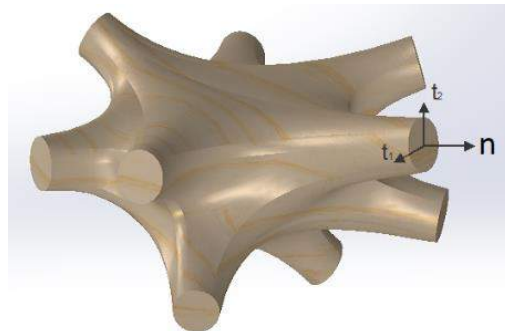
Figure 11: Local coordinates at branch's surface.

To define the boundary conditions of the model for this analysis, the face of all branches connected to the converging bars are assumed to be fixed with zero displacement along local tangential t1 and t2 directions and free to move along the normal direction. Figure 11 shows the local coordinate of one branch's surface including three orthogonal elements namely, t1, t2 and n (local normal direction).

Figure 12 shows the results of static analysis of the node before optimization. As illustrated, the maximum values obtained for the maximum von Mises stress, the maximum total displacement, the maximum energy density and mass are 55 MPa, 5e-4 mm (0.5μm), 6e3 J/m^3 and 0.85 kg, respectively.

Knowing the values of pre-optimization analysis and static characteristics of the node structure, we chose 1 kg for the mass target value, M_{target}. The resulting optimized structure can be seen in Figure 13 and the results of the optimization process are shown in Figure 14. The values obtained for the maximum von Mises stress, the maximum total displacement, and mass are 42 MPa, 3e-4 mm (0.3μm), and 0.97 kg, respectively. These values are compared in Table 3

for the node before and after optimization process. The variation of curve parameters is shown in Figure 15 before and after optimization. The optimization process was performed using genetic algorithm in MATLAB optimization toolbox with the settings as population size of 200, tournament selection method, single point crossover with rate of 0.8, adaptive feasible mutation with rate of 0.01 and 500 iterations while maintaining the threshold value of mass below 1 kg.
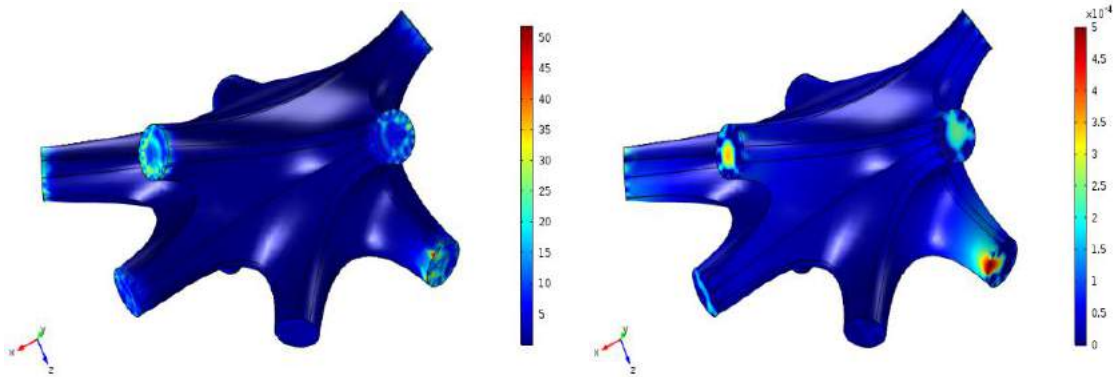
Figure 12: From left to right. Node Characteristics before Optimization: (a) Maximum von Mises Stress (MPa), (b) Maximum Total Displacement (mm).
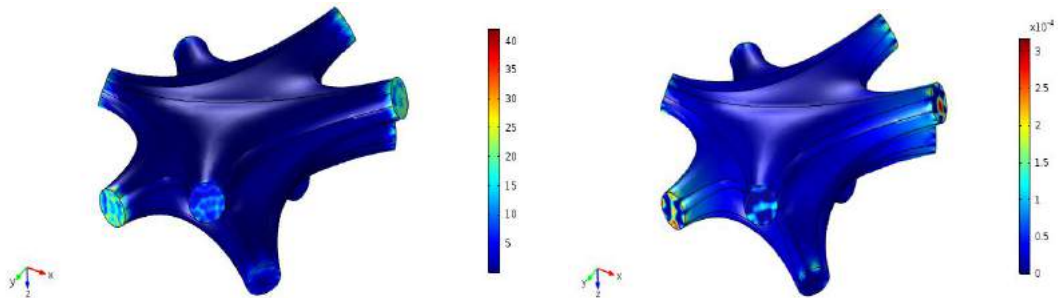
Figure 13: From left to right. Node Characteristics after Optimization: (a) Maximum von Mises Stress (MPa), (b) Maximum Total Displacement (mm).
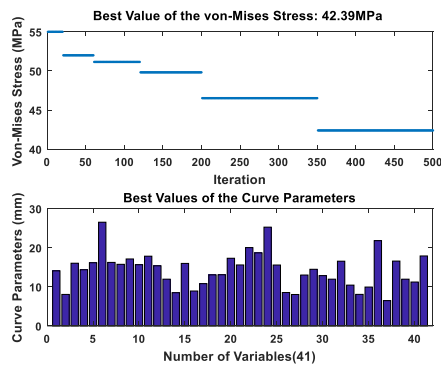
Figure 14: Upper panel: number of iterations and the best value of the objective function, lower panel: best values of the parameters.

Mechanical Characteristics	Mass (gr)	Von Mises Stress (Mpa)	Total Displacement (mm)	Strain Energy Density (J/m^3)	Minimum Safety Factor	Volumetric Strain
Before Optimization	850	55	5e-4	6e3	18.2	1e-4
After Optimization	970	42	3.291e-4	4e3	26.3	0.8e-4

Table 3: Comparison of structural characteristics before and after optimization.

It evidently appears that the structural characteristics of the node have been significantly improved after the optimization process. The decrease of 24% for the maximum von Mises stress, 34% for the maximum total displacement, 33% for the strain energy density and the increase of 24% for the minimum safety factor ensures the higher safety margin for the node.
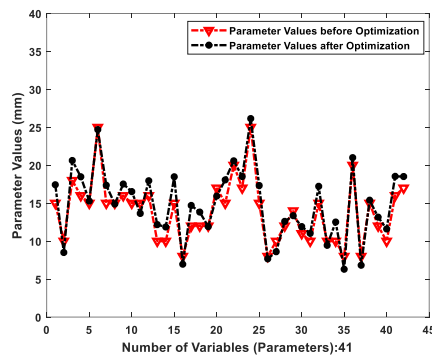
Figure 15: Variation of curve parameters, D_i's, before and after optimization.

4   FATNESS PARAMETER METHOD

This section describes the fatness parameter method for designing the node in three steps namely, node sketching, parameterization and structural optimization and can be applied to all types of nodes which belongs to the class of node as shown in Figure 2(b). The method, which is discussed in this section, is implemented using a different CAD environment in order to take advantage of its more systematic and quicker capabilities. Specifically, the following software was used: Rhinoceros (Rhino) for the design environment, Grasshopper for parametric design, Exo Wireframe for node geometric modeling, Karamba 3D for FEA, and Galapagos for optimization. The digital workflow is shown schematically in Figure 16.
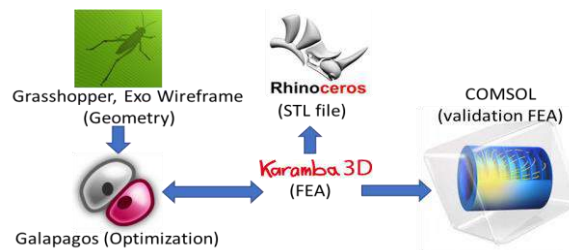
Figure 16: Overview of optimization process.

4.1 Node Sketching

As discussed earlier, the node in this research is sketched based on the information of a pre-designed SF structure. Using the dimensional information of the blank space where the SF bars are converged, the length of the node's branches and their orientation will be determined. In the fatness parameter method, the drawing of the node is done in the Rhino-Grasshopper environment. Grasshopper enables us to sketch and implement a combination of geometries in Rhinoceros software using parametric approach.

In order to start drawing of the node, firstly the intersection point is set to (0,0,0) in 3d-space and all branch points are connected to this point using line segments. To create the geometry, a Grasshopper sub-component is used, known as Exo Wireframe (part of the Exoskeleton [29] plug-in), was used to create meshes. It thickens the input lines and nodes and generates watertight meshes as output. As shown in Figure 17, it transforms the line segments into a convex hull and stitches the hulls together to create a triangular mesh node model.
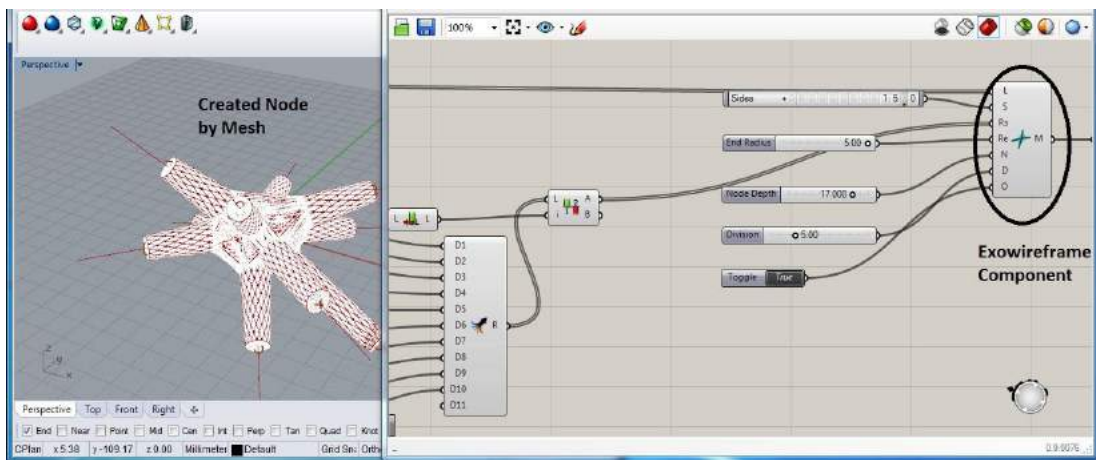
Figure 17: Exo Wireframe and generation of thickened node.
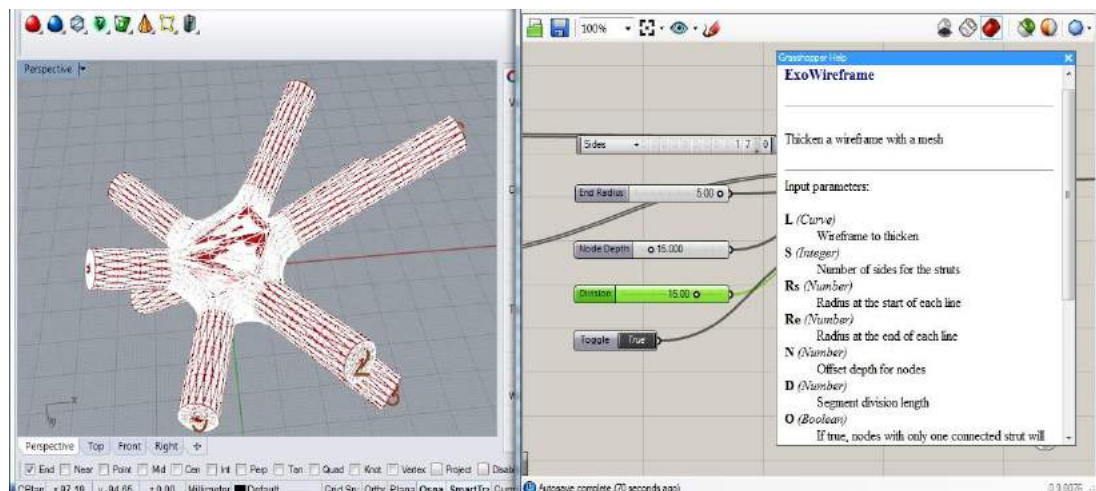
Figure 18: Elements of Exo Wireframe component.

The output of Exo Wireframe, which is shown by 'M' in the component workflow, creates the mesh in stereo-lithography (stl) format. Each of the input items is separately shown in Figure 18. Input 'L' takes the initial geometry that has been created in terms of lines and nodes in Figure 18. Subsequently, input 'S' represents the number of facets around each cylindrical or conical branch. Increasing or decreasing this item will increase or decrease the number of triangles, respectively. R_s stands for the starting radius that is variable in this design and R_e is the ending radius of each node's branch which is fixed in this design and equal to 5mm. The central fatness of the node is adjusted by the value, which is allocated to input 'N'. Input 'D' determines the division length of all polygon mesh segments, controlling the triangle mesh density along each branch.

4.2   Node Parameterization

As discussed in Section 4.1, there are some parameters that can affect the final configuration of created geometry. Parameters 'D' and 'S' will influence on the mesh structure and do not play a role on the final configuration of the node, but control the smoothness (facetted appearance) of solid node geometry. The only remaining parameters that can potentially play role on the final geometry, are N, R_s and R_e. Since the diameter of the converging bars is fixed in the SF structure, R_e will remain unchanged during the structural optimization process. Thus, two parameters, R_s and N are chosen as design variables (parameters) for changing node shape during optimization. The effects of these parameters on the geometry of the node is considered in Figures 19 and 20. Parameter 'N' will control the central fatness of the node as shown in Figure 19. Parameter R_s alters the root fatness of each node's branch individually. Figure 20 illustrates the configuration of the node, when only one of the starting radiuses has been changed.
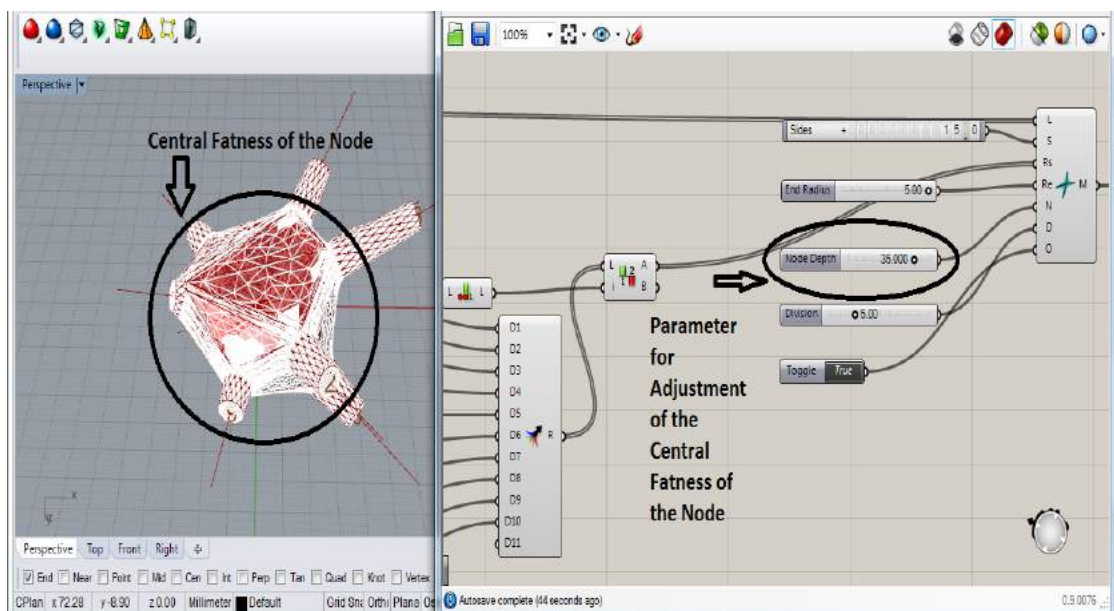
Figure 19: Effect of parameter 'N' on the central fatness of node.

The lower limit of parameters has to be constrained with a positive value like 1 mm in this case, but the upper limit of parameters has a very important role on the coherence of the mesh structure. For instance, if the assigned value of 'N' exceeds a threshold depending on the geometry of the node, the mesh tries to extend beyond the shortest branch and can cause the mesh to become undefined. For this particular node, the upper limit of R_s is chosen 5 mm, while the upper limit for 'N' can be up to 40 mm within the structural optimization process.
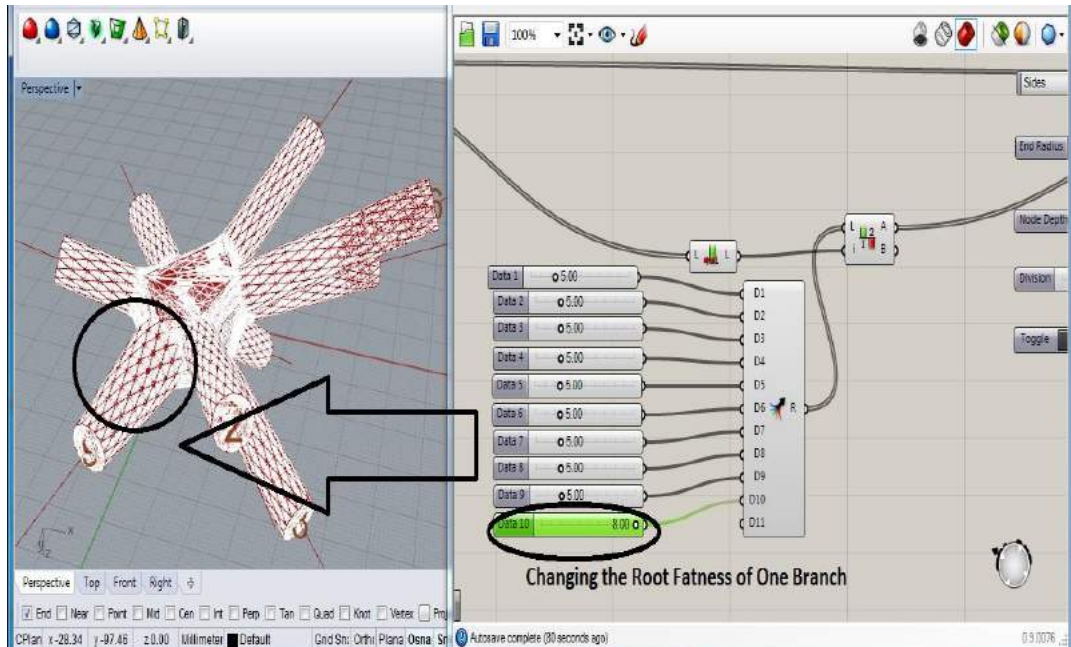
Figure 20: Effect of parameter 'R$_S$' on the root fatness of each node's branch.

4.3   Node Structural Optimization

After finding the lower and upper bounds of the parameters in the previous section, the mid-point of these bounds is set as initial values at the beginning of the optimization process. Then, one FEA is carried out to know the mechanical characteristics of the node based on the initial values. Both loads applied and boundary conditions are assumed to be the same as in the curve parameter method.

Again, the material chosen the MaragingSteel MS1 powder for EOS M280 machines. Figure 21 shows the results of static analysis using COMSOL of the node before optimization. As illustrated, the maximum values obtained for the maximum von Mises stress and the maximum total displacement are 60 MPa and 5.3e-4 mm. The value of mass is recorded 0.33 kg at this stage.
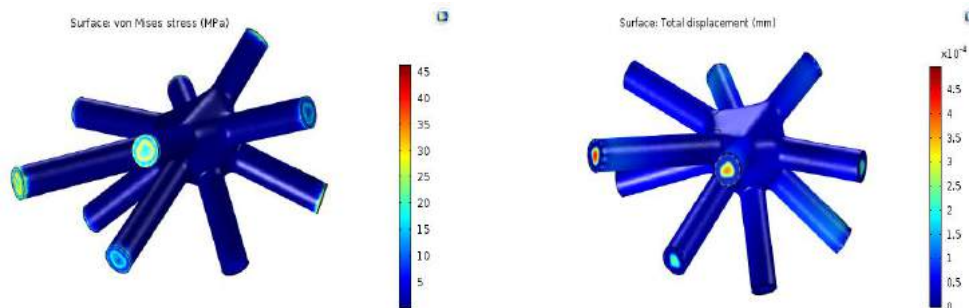
Figure 21: From left to right. Results before Optimization: (a) Maximum von Mises Stress (MPa), (b) Maximum Total Displacement (mm).
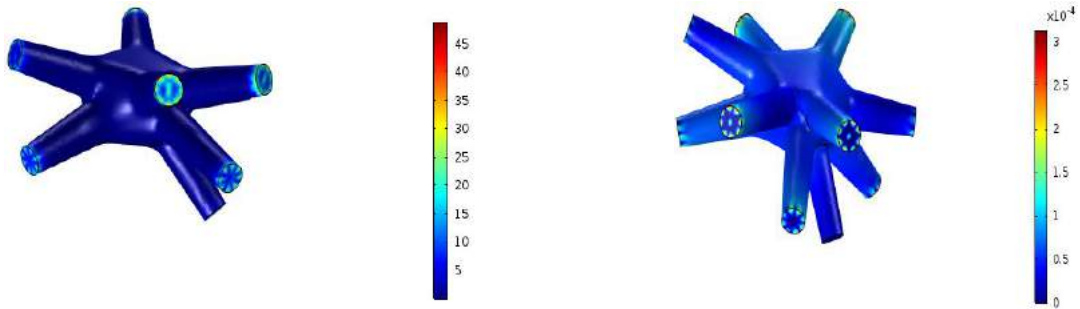
Figure 22: From left to right. Results after Optimization: (a) Maximum von Mises Stress (MPa), (b) Maximum Total Displacement (mm).

For the structural optimization, similar to the curve parameter method, maximum von Mises stress of the node is selected as the objective function with mass constraint. The target mass is chosen 1 kg for this analysis too. The resulting optimized structure is displayed in Figure 22. As seen, the maximum values obtained for the maximum von Mises stress is 45 MPa and the maximum value of total displacement decreases down to 3e-4 mm. Unlike the minimization of the structural values, the mass of node increases up to only 0.51 kg.

The FEA process was completed in Karamba, a plug-in for Grasshopper. By utilization of this plug-in, the generated meshes by Exo Wireframe component will be converted to beam and shell elements and FEA will be performed by applying the load and boundary condition as shown in Figure 23. Similar to the curve parameter method FEA model, point loads are applied at the center of each branch end-face and along the branch center-line. Nodes are constrained to displace only along the branch's center-line. Before and after optimization, the mesh models were imported into COMSOL and converted to solids, in order to perform FEA with solid elements, similar to the curve parameter method. These COMSOL FE analyses were to verify that the Karamba FEA results were correct.

Optimization was performed by the Galapagos [27] plug-in for Grasshopper; we utilized the genetic algorithm capabilities of Galapagos. The optimization parameters are defined for this component as shown in Figure 24(a) and the objective function is optimized based on altering the parameter values (see Figure 24(b)). The variation of fatness parameters is shown in Figure 25 before and after the optimization process.
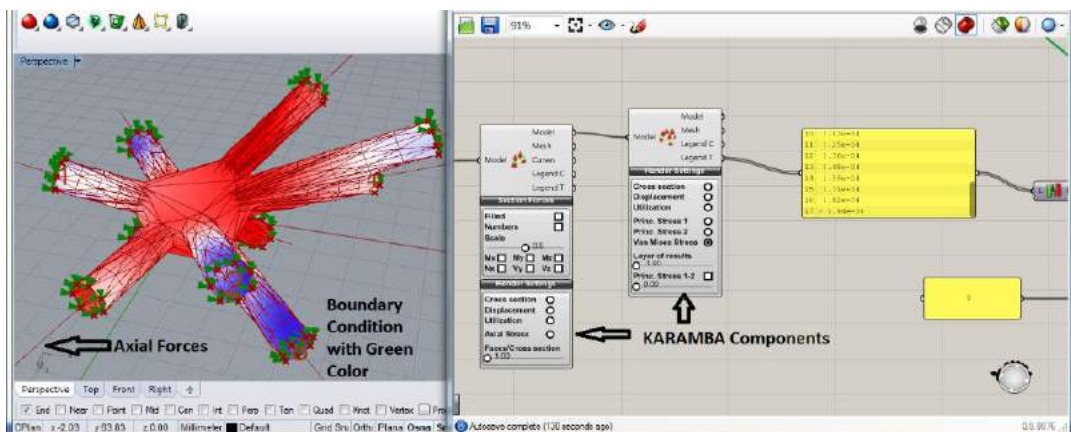
Figure 23: Karamba components for FE analysis.

The structural characteristics of the node are compared before and after optimization process in Table 4 at which one can observe the decrease of 25% for the maximum von Mises stress, 35% decrease for the maximum total displacement, 33% decrease for the strain energy density and increase of 25% for the minimum safety factor.

Mechanical Characteristics	Mass (gr)	Von Mises Stress (Mpa)	Total Displacement (mm)	Strain Energy Density (J/m³)	Minimum Safety Factor	Volumetric Strain
Before Optimization	330	60	5.3e-4	6e3	16.66	1.73e-4
After Optimization	510	40	3.00e-4	4e3	25	1.2e-4

Table 4: Comparison of structural characteristics before and after optimization.
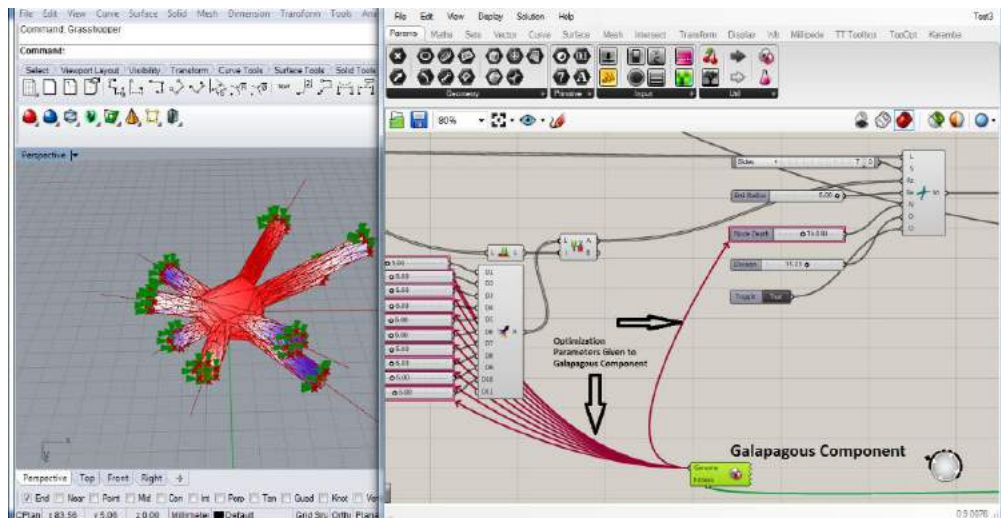
Figure 24: From left to right. Optimization by Galapagos, (a) Defining the Parameters for Galapagos Component, (b) Optimization Process using Genetic Algorithm at Galapagos-Grasshopper Interface.
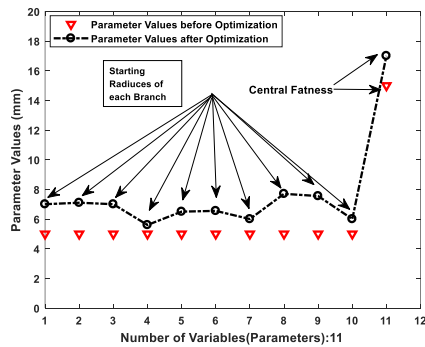
Figure 25: Variation of fatness parameters before and after optimization.

5   FUNCTIONAL TESTING AND COMPARISON

In order to determine the mechanical properties of the printed nodes using an EOS M280 metal 3D-printer, a functional experiment was conducted. This experiment aims to compare the stiffness for two nodes along their build direction. In this section, the build process of two nodes are discussed firstly and subsequently the experimental results will be described and analyzed respectively.

5.1   3D-Printed Nodes

The nodes designed by the two design methods were printed on an EOS M280 metal printer in the MaragingSteel MS1 material. The node designed with the curve parameter method is shown at the left of Figure 26, while the node from the fatness parameter method is the right. These nodes have been removed from their support structures and polished.

Figure 26: Nodes after post-processing (curve parameter node at left, fatness parameter node at right).

5.2   Experimental Results

In order to determine the approximate stiffness of the nodes along the build direction, 1% strain is applied to the same point on each node by using the point load gripper of an INSTRON tensile testing machine as shown in Figure 27 for the fatness parameter node. The nodes are fixed to the platform and the experiment is carried out three times to ensure the repeatability of the test.
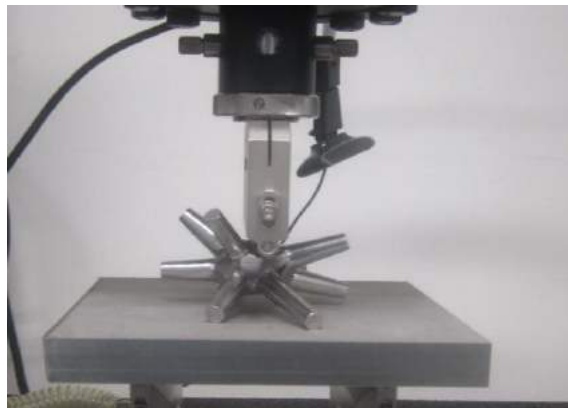
Figure 27: Applying point load by INSTRON machine to the fatness parameter node.

After applying the strain, the machine measures the output force (N) and the input extension (mm) and the corresponding force-extension curve is plotted as seen in Figure 28 for one test.
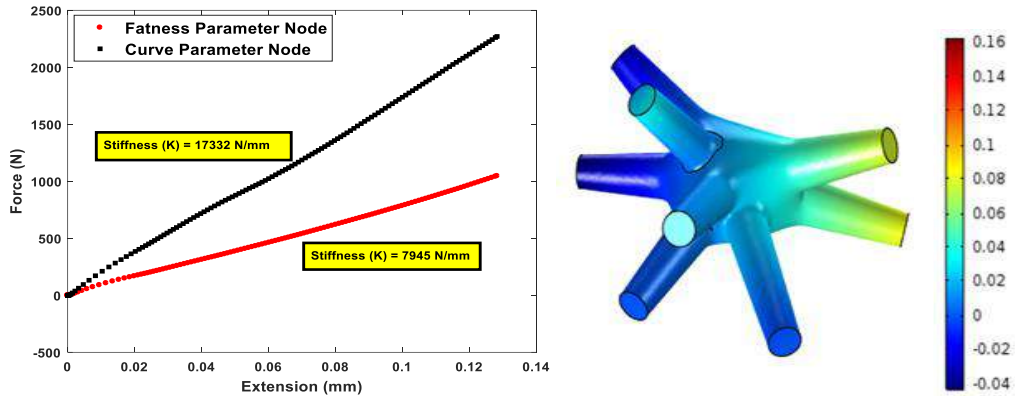
Figure 28: Experimental results: (left) force-extension graph, black line: curve parameter node, red line: fatness parameter node; (right) confirmation FEA results showing displacements.

Table 5 represents a quantitative comparison in terms of properties and characteristics of the two nodes in this study. As expected, the curve parameter node reveals larger average stiffness of 17100 N/mm in comparison with the lower value of 7754 N/mm for the fatness parameter node due to the greater amount of material along the build direction. However, from the mass efficiency point of view, the average stiffness/weight ratios of the two nodes were remarkably similar, which indicates that the optimization methods made significant progress in the right direction. The dimensions of the nodes were 100×97×70 mm (length, width, height).

Parameters	Approximate Sketch Time (hrs)	Output Format of the Sketch	Approximate Build Time (hrs)	Average Stiffness along Build Direction (N/mm)	Average Stiffness/Weight Ratio (N/kg.mm)
Fatness Parameter Node	≈0.15	Mesh (Converted to Solid using Secondary Software)	≈12	7754	15508
Curve Parameter Node	≈1	Solid	≈15	17100	15600

Table 5: Quantitative comparison between two nodes after manufacturing.

An overall qualitative comparison between the two design methods is presented in Table 6, assessing the advantages and disadvantages of each. The curve parameter method has advantages in that a solid model is constructed that leads to solid FEA models for optimization. However, this comes at the cost of a semi-automated method that requires the designer to manually select branches to connect with splines and spline surfaces. In contrast, the fatness parameter method is automated, but works with a mesh model. The resulting FEA and optimization models are less precise as a consequence. Furthermore, the curve parameter method enables a greater number of

design variables, compared to the fatness parameter method, that offers more shape controls which could be valuable in optimizing node designs.

Some final comments can be made regarding the optimized node designs and the design methods. The first observation is that design time was significant reduced from 5-10 hours to 15 minutes, or 1 hour, with the fatness parameter or curve parameter methods, respectively. Optimization results appear to be highly dependent on initial designs. This indicates that the genetic algorithm parameters were not optimized and that better results could be obtained with either better parameters or different optimization methods. As a consequence, the design methods should not be directly compared based on the optimized nodes. For example, it is not appropriate to conclude that the fatness parameter method yields lighter nodes. Finally, the fatness parameter optimization method did not seem to suffer from the usage of a shell (surface) FEA model, since optimization proceeded successfully and yielded a stiffness/weight ratio similar to that of the curve parameter method.

	Pros	*Cons*
Curve Parameter	Effective at generating node designs Solid model Solid FEA elements More parameters (ex: 41 vs 11)	Manual curve sketching, surface construction, knitting Node surface has C0 continuity along the knit curves, thus are not smooth
Fatness Parameter	Effective at generating node designs Automated model construction after sketching branches Smooth shapes	Surface model Shell FEA elements Less shape control (fewer parameters)

Table 6: Comparison between the two node design methods.

6   CONCLUSION

In this article, two variations of the form-finding methods for SF nodes were demonstrated in terms of structural optimization. The curve parameter design method was semi-automated, with the designer responsible for constructing a surface model, based on a defined procedure. The other method, the fatness parameter method, was automated based on an automated meshing approach. An important consequence was that the resulting model was a mesh, not a solid, which required a shell-based FEA model for structural analysis. Optimization procedures were developed for the design methods. Nodes were designed using both methods. They were fabricated using a metal powder bed fusion additive manufacturing process, then tested physically for their stiffness characteristics. The optimized nodes had different masses and stiffnesses, but virtually identical mass efficiency characteristics, indicated by their stiffness/mass ratios. The advantages and disadvantages of the design methods were summarized in the paper.

Future work should focus on developing an automated curve parameter method. This should be possible by applying an algorithm to recognize the closest node branches and constructing the curves and surfaces automatically. Additionally, the optimization procedures should be improved by developing better genetic algorithm parameters, or allowing additional iterations, and by exploring alternative optimization methods.

7   ORCID

Vahid Hassani, https://orcid.org/0000-0001-6724-2520.
Zubin Khabazi, https://orcid.org/0000-0002-8956-9679.
Felix Raspall, http://orcid.org/ 0000-0002-7213-4572.
Carlos Banon, https://orcid.org/0000-0002-7408-5639.
David W. Rosen, https://orcid.org/0000-0002-7257-9395.

REFERENCES

[1]   Abele, E.; Fujara, M.: Simulation-Based twist drill design and geometry optimization, CIRP Annals-Manufacturing Technology, 59, 2010, 145-150. http://doi.org/10.1016/j.cirp.2010.03.063

[2]   Arora, J. S.: Introduction to optimum design, Fourth Edition,Elsevier, 2017. http://doi.org/10.1016/C2009-0-61700-1

[3]   Bendsoe, M. P.; Sigmund, O.: Topology optimization: theory, methods and applications, Second Edition, Springer, 2003. http://doi.org/10.1007/978-3-662-05086-6

[4]   Bletzinger, K. U.; Ramm, E.: A general finite element approach to the form finding of tensile structures by the updated reference strategy, International Journal of Space Structures, 14, 1999, 131-145. http://doi.org/10.1260/0266351991494759

[5]   Buelow, P. V.; Falk, A.; Turrin, M.: Optimization of structural form using a genetic algorithm to search associative parametric geometry, Structures and Architecture, 2010, 699-706. http://doi.org/10.1201/b10428-93

[6]   Clune, R.; Kelliher, D.; Robinson, J. C.; Campbell, J. S.: NURBS Modelling and structural shape optimization of cardiovascular stents, Structural Multidesciplinary Optimization, 50, 2014, 159-168. http://doi.org/10.1007/s00158-013-1038-y

[7]   Ding, C.; Seifi, H.; Dong, S.; Xie, Y. M.: A new node-shifting method for shape optimization of reticulated spatial structures, Engineering Sructures, 152, 2017, 727-735. http://doi.org/10.1016/j.engstruct.2017.09.051

[8]   Furuya, H.: Concept of deployable tensegrity structures in space application, International Journal of Space Structures, 7, 1992, 143-151. http://doi.org/10.1177/026635119200700207

[9]   Galjaard, S.; Hofman, S.; Ren, S.: New opportunities to optimize structural designs in metal by using additive manufacturing, In: Advances in Architectural Geometry, 2014, 79-93. http://doi.org/10.1007/978-3-319-11418-76

[10] Gan, B. S.; Zhang, J.; Nguyen, D.-K.; Nouchi, E.: Node-Based genetic form-finding of irregular tensegrity structures, Computers and Sructures, 159, 2015, 61-73. http://doi.org/10.1016/j.compstruc.2015.07.003

[11] Geiger, D. H.; Stefaniuk, A.; Chen, D.: The design and construction of two cable domes for the korean olympics, Shells, Membranes and Space Frames, Proceedings of IASS Symposium,Osaka, Japan, 1986, 265-272.

[12] Gibson, I.; Rosen, D. W.; Stucker, B.: Additive manufacturing technologies: rapid prototyping to direct digital manufacturing, Second Edition, Springer, 2010. http://doi.org/10.1108/aa.2012.03332baa.010

[13] Hanaor, A.: Double-Layer tensegrity grids as deployable structures, International Journal of Space Structures, 8, 1993, 135-145. http://doi.org/10.1177/0266351193008001-214

[14] Haug, E.; Powell, G. H.: Analtical shape finding for cable nets, In: Proceedings of the 1971 IASS Pacific Symposium Part II on Tension Structures and Space Frames, Tokyo, Japan, 1972, 83-92.

[15] Kang, P.; Youn, S.-K.: Isogeometric shape optimization of trimmed shell structures, Building Engineering, 53, 2016, 825-845. http://doi.org/10.1007/s00158-015-1361-6

[16] Kociecki, M.; Adeli, H.: Shape optimization of free-form steel space-frame roof structures with complex geometries using evolutionary computing, Engineering Applications of Artificial Intelligence, 38, 2015, 168-182. http://doi.org/10.1016/j.engappai.2014.10.012

[17] Lee, S. J.: A form-finding technique for three-dimensional spatial structures, Architectural Research, 15, 2013, 207-214. http://doi.org/10.5659/AIKAR.2013.15.4.207

[18] Linn, R. V.; Espath, L. F. R.; Awruch, A. M.: Optimal shape of axisymmetric solids using NURBS and automatic differentiation, Applied Mathematical Modelling, 38, 2014, 1385-1402. http://doi.org/10.1016/j.apm.2013.08.024

[19] Marco, O.; Rodenas, J. J.; Albelda, J.; Nadal, E.; Tur, M.: Structural shape optimization using cartesian grids and automatic H-Adaptive mesh projection, Structural Multidesciplinary Optimization, 58, 2018, 61-81. http://doi.org/10.1007/s00158-017-1875-1

[20] Mueller, C. T.: 3D printed structures: challenges and opportunities, Structure, 54, 2016.

[21] Noel, F.; Leon, J. C.; Trompette, P.: Shape optimization of three-dimensional parts based on a closed loop between structure analysis and geometric modeling, Engineering with Computers, 11, 1995, 114-121. http://doi.org/10.1007/BF01312205

[22] Paul, C.; Lipson, H.; Valero-Cuevas, F.: Design and control of tensegrity robots for locomotion, IEEE Transactions on Robotics, 22, 2006, 944-957. http://doi.org/10.1109/TRO.2006.878980

[23] Preisinger, C.: Linking structure and parametric geometry, Architect Design, http://doi.org/10.1002/ad.1564, 83, 2013, 110-113. http://doi.org/10.1002/ad.1564

[24] Raspall, F.; Banon, C.: vMesh: How to print architecture?, SIGraDi 2016, XX Congreso de la Sociedad Ibero-americana de Grafica Digital 9-11, Buenos Aires, Argentina, 2016. http://doi.org/10.5151/despro-sigradi2016-771

[25] Raspall, F.; Banon, C.: 3D-printing architecture: Towards functional space frames, CAADRIA 2018, v 1, p 215-224, Beijing, May 17-18, 2018.

[26] Rosen, D. W.: What are principles for design for additive manufacturing?, 1st International Conference on Progress in Additive Manufacturing, 2014. http://doi.org/10.3850/978-981-09-0446-3_027

[27] Rutten, D.: Evolutionary principles applied to problem solving, https://www.grasshopper3d.com/m/blogpost?id=2985220%3ABlogPost%3A99500, 2010.

[28] Schek, H. J.: The force density method for form finding and computation of general networks, Computer Methods in Applied Mechanics and Engineering, 3, 1974, 115-134. http://doi.org/10.1016/0045-7825(74)90045-0

[29] Stasiuk, D.: Exoskeleton, https://www.grasshapper3d.com/group/exoskeleton, 2014.

[30] Veenendaal, D.; Block, P.: An overview and comparison of structural form finding methods for general networks, International Journal of Solids and Structures, 49, 2012, 3741-3753. http://doi.org/10.1016/j.ijsolstr.2012.08.008

[31] Wachsmann,K.: The turning point of building: structure and design, Reinhold Publication Corporation, 1961.

[32] Wang, X.; Zhou, J.; Hu, Y.: A physics-based parameterization method for shape optimization, Computer Methods Applied in Mechanical Engineering, 175, 1999, 41-51. http://doi.org/10.1016/S0045-7825(98)00318-1

[33] Weiss, D.: Feature-Based spline optimization in CAD: a step towards geometry-based structure creation, Structural Multidesciplinary Optimization, 42, 2010, 619-631. http://doi.org/10.1007/s00158-010-0521-y

[34] Winslow, P.; Pellegrino, S.; Sharma, S. B.: Multi-Objective optimization of free-form grid structures, Structural and Multidesciplinary Optimization, 40, 2010, 257-269. http://doi.org/10.1007/s00158-009-0358-4